International Specialty Conference on Cold-Formed Steel Structures

(2010) - 20th International Specialty Conference on Cold-Formed Steel Structures

Nov 3rd, 12:00 AM

Impact of Corner Radius on Cold-formed Steel Member Strength

V. Zeinoddini

B. W. Schafer

Follow this and additional works at: https://scholarsmine.mst.edu/isccss

Part of the Structural Engineering Commons

Impact of corner radius on
cold-formed steel member strength

V. Zeinoddini[1] and B.W. Schafer[2]

Abstract

The objectives of this paper are to explore (a) how corners of cold-formed steel members are included or ignored in current design methods, and (b) the effectiveness of recent proposals for modifying the strength prediction for local buckling to account for corners. The impact of round corners is examined on the behavior and strength of isolated elements and on full members using material and geometric nonlinear collapse analysis with shell finite elements in ABAQUS. Comparisons between the available methods and the nonlinear finite element analysis are completed to explore the regimes in which the methods are accurate, as well as when they are deficient. The current approach in the main Specification of AISI-S100-07, which applies no reductions regardless of corner size, is demonstrated to be unconservative. Initial recommendations for the design of sections with large corner radius by effective width and direct strength methods are provided.

1   Introduction

The formation of cold-formed steel sections requires cold bending of the sheet steel strip. This bending introduces round corners into the cross-section, along with a relatively complex state of residual stresses and strains: Moen and Schafer 2008, Gao and Moen 2010. The longstanding effective width method of design uses flat plate buckling solutions as its core tool for strength prediction, as a result their have always been questions related to how to handle the round corners in design (e.g., Marsh 1997). This paper addresses the impact of corners in elements, and in members, and provides preliminary recommendations for improving current design methods.

---

[1] Graduate Research Assistant, Department of Civil Engineering, Johns Hopkins University, Baltimore, MD, USA (vahidzm@jhu.edu)
[2] Professor and Chair, Department of Civil Engineering, Johns Hopkins University, Baltimore, MD, USA (schafer@jhu.edu)

2   Current design

According to the effective width method, as implemented in the main body of the AISI Specification (AISI-S100-07), the strength of a cross section is obtained by finding the effective width of the flat part of each element and then forming the effective area as the sum of the effective flats plus the corners. The corners are always assumed to be fully effective. This creates a false optimal design: sections comprised of all corners are always fully effective. Eurocode uses a modestly different implementation of the effective width method employing a notional flat width that includes the actual flat width plus a portion of the corners (EN-1993-1-3). This approach modestly complicates design.

The direct strength method of Appendix 1 of AISI-S100-07 does not separate the cross-section into flats and corners since full cross-section local buckling analysis is used as the basis, instead of actual or notional flats connected to plate buckling solutions. Reductions are applied to the full section and local buckling may be triggered by the flats, the corners, or any combination thereof. It is worth noting that even this approach has its limits. For extremely large corner radii the behavior may be driven by buckling within the shell-like large corners, instead of the plate-like flats; in this case, the post-buckling may be sharply reduced.

Recently, in support of AISI Specification development, an improved version of the effective width method has been proposed by committee member Robert Glauz. The proposed method continues the AISI main Specification convenience of only reducing the flat portions of the section, but modifies the plate buckling coefficient (k) to account for the reduced capacity due to large rounded corners. The plate buckling stress for any flat of width b, thickness, t, material modulus E, and Poisson's ratio v, is:

$$f_{cr} = k \frac{\pi^2 E}{12\left(1 - v^2\right)} \left(\frac{t}{b}\right)^2$$

After studying elastic buckling solutions Robert Glauz proposed that the plate buckling coefficient, k, should be reduced as follows:

$$k_{reduced} = \left(1.08 - 0.02 \frac{r_1}{t}\right)\left(1.08 - 0.02 \frac{r_2}{t}\right)k$$

where t is the thickness and r_1 and r_2 are the radius of the corners. This approach will be referred to as the "reduced k method" in this paper.

3 Behavior of elements

In this section the effect of corner radius on the strength of isolated elements, both stiffened and unstiffened, is investigated using nonlinear finite element analysis, and compared with available design methods.

3.1 Stiffened elements

Consider a stiffened element (supported on both sides), but with corner radius at its edges, as shown in Figure 1. Here we examine a stiffened element where the centerline out-to-out width, b_o, is held constant as the centerline corner radius, r, is varied (thus in turn varying the flat width, b).
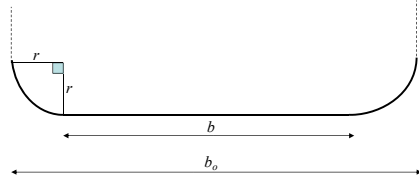

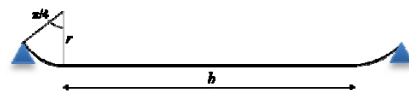Figure 1: stiffened element in a section   Figure 2: isolated stiffened element

To isolate the stiffened element from the section the selected model, Figure 2, includes half of the corner radius on each edge. The resulting area, A, is:

$$A = \left(b + \tfrac{1}{2}r\pi\right)t = \left(b_o - (2 - \tfrac{1}{2}\pi)r\right)t$$

As can be observed from the equation, the area of the element decreases as the radius increases. (If the full corner is included the area will increase with r).

If the effective width method, as implemented currently in AISI-S100-07, is employed for the strength prediction of this element alone, then:

$$P_{n1} = \left(\rho b + \tfrac{1}{2}r\pi\right)tf_y$$

where f_y is the yield stress and ρ is the effectiveness of the flat portion, defined by Winter's equation as:

$$\rho = (1 - 0.22/\lambda)/\lambda \text{ for } \lambda > 0.673, \text{ and}$$

$$\rho = 1 \text{ for } \lambda \leq 0.673, \text{ and } \lambda = \sqrt{f_y/f_{cr}}$$

where f_{cr} is the buckling stress for the element, defined previously. If the usual k = 4.0 for stiffened elements is employed, then the preceding is the traditional AISI effective width approach. However, if the reduced k equation is employed, f_{cr}, λ, ρ, and finally P_n are modified – thus the reduced k method provides an alternative prediction, P_{n2}, with the same expression as P_{n1} but a revised ρ.

The essential feature of the direct strength method approach is the reduction of the entire member, as opposed to just the flats. Such an approach provides a strength prediction for an isolated element in the following form:

$$P_{n3} = \rho\left(b + \tfrac{1}{2} r\pi\right) t f_y$$

The "effectiveness" may use Winter's equation for ρ, but the f_{cr} as used in λ and in the determination of ρ should be for the full element including corners (a proper section analysis) not just the flats.

3.1.1 Stiffened element comparison with FE
Nonlinear collapse analysis was conducted with ABAQUS to study the ultimate strength of the stiffened element model (Figure 2). The model utilized simply supported boundary conditions (out of plane displacement on the edges were restrained), geometric imperfections in the shape of the first local buckling mode with a maximum magnitude = $0.34t$ = 0.01in. (Schafer and Peköz 1998), and an elastic perfectly-plastic stress-strain relation with E=29500 ksi, $v=0.3$, and f_y=33 ksi. A range of elements, 0.03 in. thick, with different width and corner radii: b_o/t =60, 100, 120, 250, and 500; and r/t = 0, 4, 7, 10, 15, and 20, are analyzed. The length of the model, a, is four times the total width (a/b_o=4).

To compare the effectiveness of strength predictions P_{n1} (traditional effective width ignoring corners) and P_{n3} (direct strength applied to an element including corners) the ρ required for the P_n predictions to match the observed collapse strengths in the ABAQUS analyses were back-calculated and the results plotted in Figure 3. The required reduction for P_{n3} to exactly match the observed ABAQUS results is nearly identical to Winter's equation. For the traditional effective width method modifications are needed in ρ, as at a given slenderness the change in corner radius has a significant impact on the needed ρ.
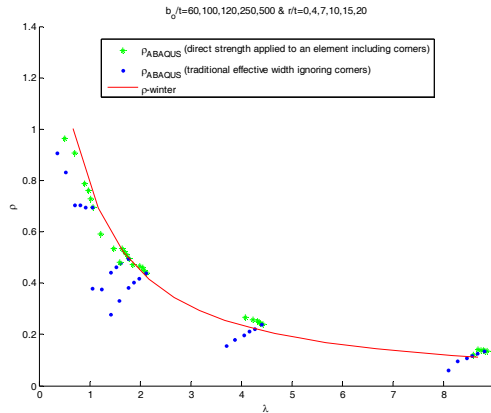
Figure 3: comparison of local reduction factor derived from ABAQUS for whole cross section and for the flat part

A more direct comparison of the finite element collapse strength with the predictions: P_{n1} (traditional effective width ignoring corners) and P_{n3} (direct strength applied to an element including corners) is provided in Figures 4 for P_{n1} and Figures 5 for P_{n3}. In the provided results b_o is set to 3.6 in. (Figures 4a and 5a) and 7.5 in. (Figures 4b and 5b) $t = 0.03$ in. and r/t is varied from 0 to 20. The traditional effective width prediction, P_{n1}, becomes progressively unconservative for large r/t, and in the studied cases excessively unconservative for r/t in excess of 10. The direct strength style prediction, P_{n3} (applied to just the element and corner) provides a reliable and conservative prediction; though at $r/t = 20$ in the $b_o=3.6$ in. case is modestly unconservative.
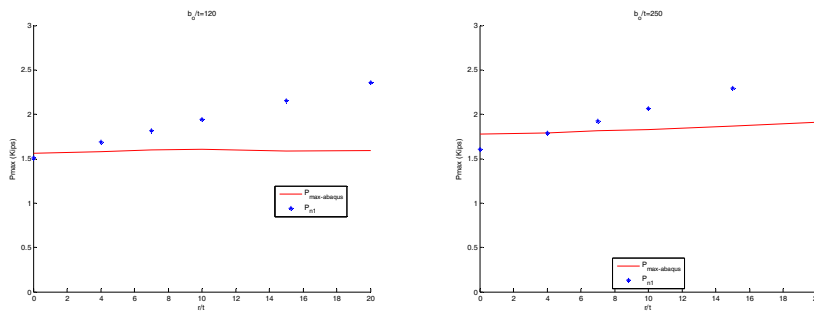

a)   b)

Figure 4: comparison between ABAQUS results and P_{n1} (traditional effective width ignoring corners). a) b_o=3.6 in., b) b_o=7.5 in.
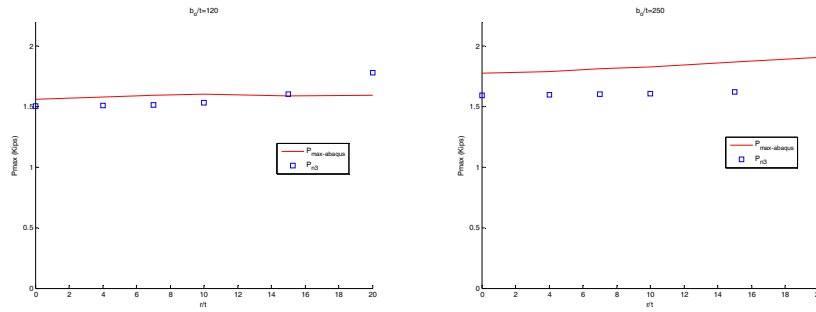
a)   b)

Figure 5: comparison between ABAQUS results and P_{n3} (direct strength applied to an element including corners). a) b_o=3.6 in., b) b_o=7.5 in.

3.1.2   Reduced k method for stiffened elements

Consider now the reduced k method, as described in Sections 2 and 3.1, and embodied in the strength prediction, P_{n2}. Figure 6 extends the studies on b_o = 3.6 and 7.5 in. stiffened elements to the reduced k method and compares them with both ABAQUS and the P_{n1} predictions. The trend towards unconservative predictions as r/t increases is decreased using the reduced k method when compared with the P_{n1} predictions. Purely from a strength standpoint, the result is encouraging halving the error (or better) up to r/t of 20.
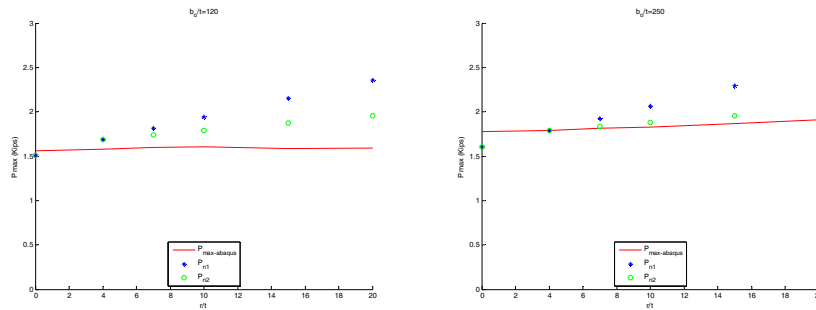
a)   b)

Figure 6: Comparison between the results of ABAQUS, reduced k method, and P_{n1}. a) b_o=3.6 in., b) b_o = 7.5 in.

A wider parametric study is also conducted on the reduced k method. ABAQUS predicted collapse strengths for b_o of 1.8, 3 and 7.5 in. are all compared to P_{n2} for increasing r/t in Figure 7. The reduced k method follows the same basic

trend as the expected strength; however, the method becomes more unconservative as radius increases, suggesting limits exist to the strategy.
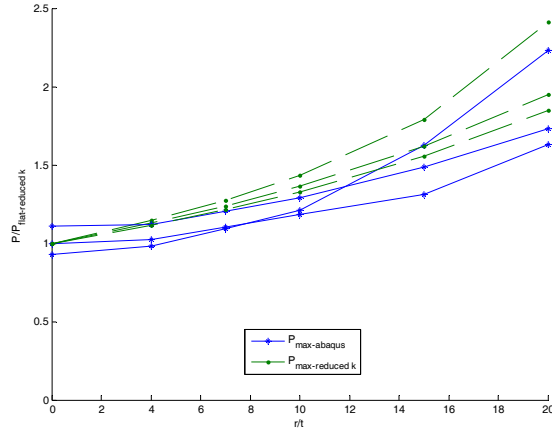

Figure 7: comparison of ABAQUS result with reduced k method (P_{n2})

Given the potential promise of the reduced k method additional analysis is conducted to investigate the $k_{reduced}$ expression directly. Since f_{cr} is defined for the flat width, b, then the plate buckling coefficient, k, may be back-calculated from an elastic buckling ABAQUS analysis and compared with $k_{reduced}$ as provided in Figure 8 for $b_o = 1.8$, 3 and 7.5 in., $t = 0.03$ in., and r/t varied from 0 to 20. As Figure 8 shows, $k_{reduced}$ provides an average reduction when compared to k's back-calculated from the actual buckling stresses. Dependence of k on both b/t and r/t is observed, but the b/t dependence is ignored in $k_{reduced}$.

Since the ultimate objective of $k_{reduced}$ is to provide an improved strength prediction then a more meaningful comparison may be to the back-calculated k value that would generate a P_{n2} prediction equal to an ABAQUS collapse analysis. This comparison is provided in Figure 9 and in this context $k_{reduced}$ is observed to be an upperbound solution and again missing an observable dependence on b/t.
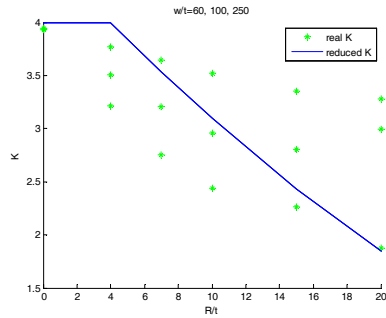
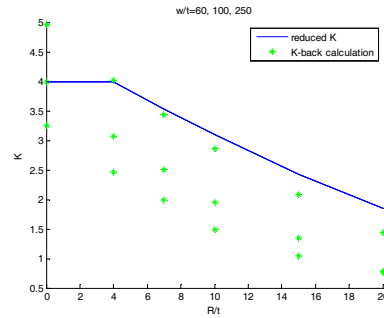Figure 8: compare k's derived from ABAQUS **buckling** analysis and reduced k method

Figure 9: compare k's derived from ABAQUS **collapse** analysis and reduced k method

3.2 Unstiffened elements

In this section finite element studies and comparisons are completed for unstiffened elements similar to those reported on stiffened elements in the previous section. However, in general, the behavior is more complicated and solutions are difficult to generalize. The basic unstiffened element is provided in Figure 10 and the idealized and isolated model with ½ of the corner included is detailed in Figure 11. The traditional effective width strength prediction is:

$$P_{n1} = \left(\rho b + \tfrac{1}{4} r \pi \right) f_y$$

where ρ follows Winter's equation as previously given in Section 3.1 and f_{cr} is suitably updated with the unstiffened element $k = 0.425$. A reduced k method strength prediction, P_{n2}, utilizes the same functional form as P_{n1}, but with $k_{reduced}$ replacing k in f_{cr}. The direct strength style expression for an unstiffened element with a corner follows:

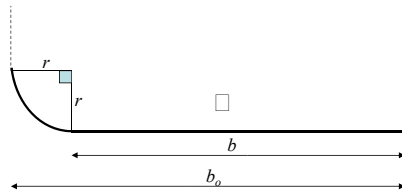$$P_{n3} = \rho \left(b + \tfrac{1}{4} r \pi \right) f_y$$

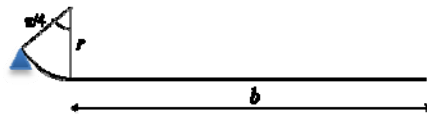Figure 10: unstiffened element in a section

Figure 11: isolated unstiffened element

3.2.1 Unstiffened element comparison with FE

A series of nonlinear finite element models of unstiffened elements are analyzed to collapse using ABAQUS. The models utilize simply supported boundary conditions on the ends and the side that includes the corner, the opposite side has free boundary conditions. Geometric imperfections in the shape of the first local buckling mode with a maximum magnitude of $0.94t = 0.028$ in*., where $t =$ 0.03 in. (according to [Schafer and Peköz 1998] for type 2 element out-of-straghtness imperfections), and an elastic perfectly-plastic stress-strain relation with E=29500 ksi, v=0.3, and f_y=33 ksi are employed. Models are completed at b_o = 0.9, 1.8, 3.6, and 7.5 in. and for each b_o the r/t is varied from 0 to 20. The length of the models is constant at four times the total width (a/b_o=4). Results for the ABAQUS collapse analysis are compared to P_{n1} and P_{n3} in Figures 12.
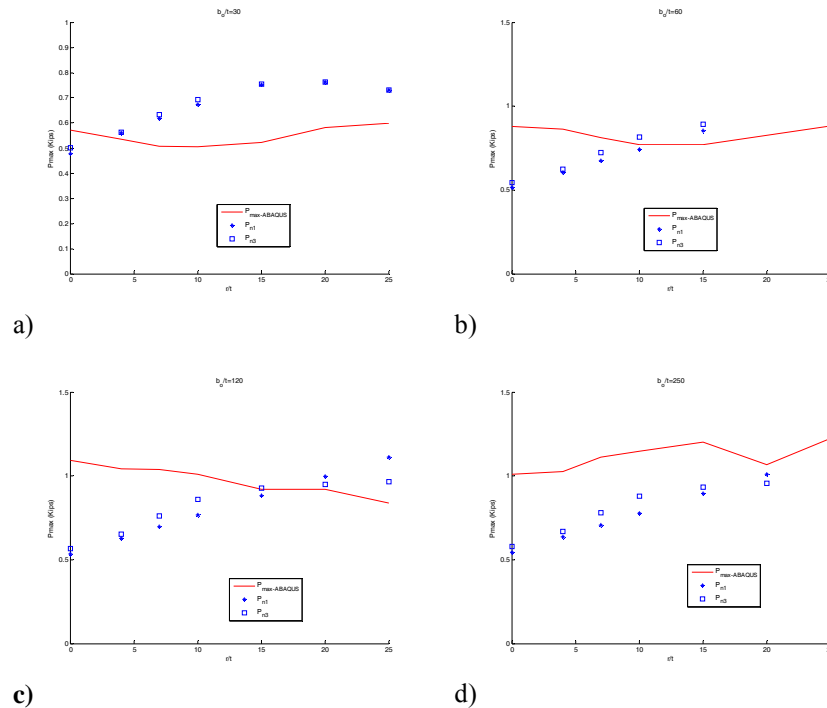

a)

b)

c)

d)

Figure 12: Comparison between the results of ABAQUS, P_{n1} (traditional effective width ignoring corners) and P_{n3} (direct strength applied to an element including corners) for unstiffened elements.:
a) b_o = 0.9 in., b) b_o = 1.8 in., c) b_o = 3.6 in., d) b_o = 7.5 in.

Figure 12 demonstrates that agreement between collapse strength as predicted by ABAQUS and P_{n1} and/or P_{n3} is relatively poor. For stocky unstiffened elements (Figure 12a) P_{n1} and P_{n3} provide generally unconservative predictions, for slender unstiffened elements (Figure 12d) P_{n1} and P_{n3} provide generally conservative predictions and for intermediate slenderness (Figures 12b and 12c) the agreement is better but trends with respect to increasing r/t predicted by P_{n1} and P_{n3} are not generally observed in the ABAQUS collapse analysis. Since the P_{n1} models never reduce the corners it is no surprise that for large corner radius ($\sim r/t > 15$) the P_{n1} models provide strength predictions in excess of P_{n3} and are unconservative compared with the collapse analysis strength from ABAQUS.

As an aside, the plastic strain at collapse for a typical ABAQUS model of an unstiffened element is provided in Figure 13. Ideally, the yielding would be further from the ends of the member. Additional work on the modeling of the unstiffened elements may be beneficial before drawing final conclusions on the adequacy of the design methods.
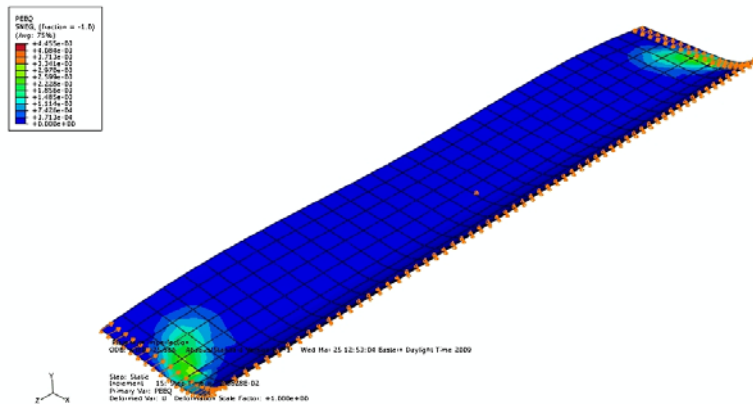

Figure 13: plastic strain at the peak load for an unstiffened element

3.2.2 Reduced k method for unstiffened elements

The reduced k method (and related strength prediction P_{n2}) may also be employed to predict the strength of unstiffened elements. Figures 14 and 15 provide corollaries to the studies of Figures 12a and 12b for the reduced k method. Figure 14 provides comparison to ABAQUS and P_{n3} (direct strength), while Figures 15 provide comparisons to ABAQUS and P_{n3} (effective width). The reduced k method performs largely similar to the direct strength style prediction of P_{n3}. Figure 15b provides the most compelling comparison, indicating the advantage of the reduced k method over the traditional approach (P_{n1}) which is linearly and incorrectly increasing with higher r/t.
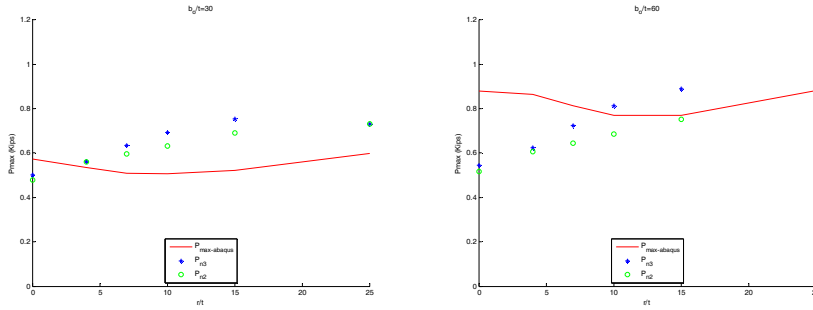
a)   b)

Figure14: Comparison between the results of ABAQUS, reduced k method, and
P$_{n3}$ for unstiffened elements. a) b_o = 0.9 in., b) b_o = 1.8 in.
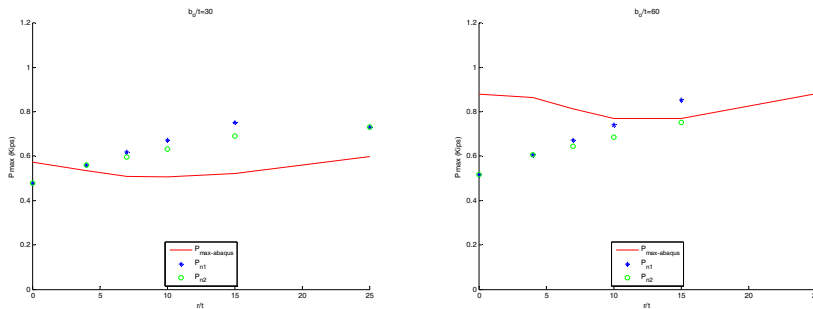
a)   b)

Figure15: Comparison between the results of ABAQUS, reduced k method, and
P$_{n1}$ for unstiffened elements. a) b_o = 0.9 in., b) b_o = 1.8 in.

4   Behavior of members

In this section the effect of corner radius on the strength of full cross sections is
investigated. Two types of cross sections are considered: square hollow section
tubes composed of four stiffened elements, and equal leg angles, composed of
two unstiffened elements. Corner radius in the studied sections is varied.

4.1   Members with stiffened elements (i.e. tubes):
Consider a simply supported[3] square hollow section stub column (a/b_o = 2)
under compressive loading with centerline out-to-out width, b_o, of 3.6 in. or 7.5

---

[3] all nodes at the end cross-section of the member are restricted from translation,
thus this is a locally simply-supported, warping fixed, boundary condition.

in., t = 0.03 in., and modeled as elastic-perfectly plastic with E = 29500 ksi, v = 0.3, and f_y = 33 ksi. Initial imperfections are considered as the first buckling mode shape with magnitude of 0.34t (Schafer and Peköz 1998). Corner radius is varied from 0 to 25 times the thickness. The strength of these members is obtained using finite element collapse modeling in ABAQUS and compared in Figure 16 with (a) strength prediction from the effective width method in the main Specification of AISI-S100-07, P_{n2}, and (b) strength prediction from the direct strength method in Appendix 1 of AISI-S100-07, P_{n3}.

For the studied square hollow section member both the effective width (P_{n1}) and direct strength (P_{n3}) provide modestly unconservative solutions. However, the direct strength (P_{n3}) predictions follow the same pronounced nonlinear trends observed in the ABAQUS results, while the effective width method essentially assumes a linear change in strength as a function of r/t – a trend not borne out by the ABAQUS results.
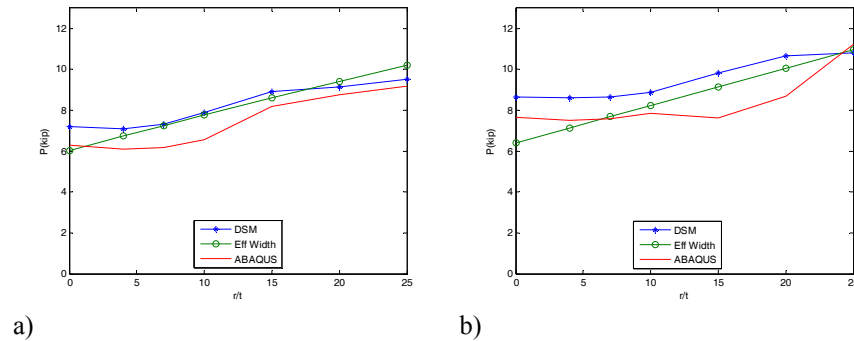

a)   b)

Figure16: strength of tube members under axial compression.
a) b_o = 3.6 in. wide, b) b_o = 7.5 in. wide

4.2   Members with unstiffened elements (i.e. angles):

In this section a simply supported[3] angle section stub column (a/b_o = 2) under compressive loading with centerline out-to-out width, b_o, of 0.9 in., 1.8 in., 3.6 in. or 7.5 in., t = 0.03 in., and modeled as elastic-perfectly plastic with E = 29500 ksi, v = 0.3, f_y = 33 ksi is considered. Initial imperfections are considered in the shape of the first buckling mode with a magnitude of 0.94t (Schafer and Peköz 1998). Corner radius is varied from 0 to 25 times the thickness. The strength of these members is obtained using finite element collapse modeling by ABAQUS and compared in Figure 17 with (a) strength prediction from the effective width method in the main Specification of AISI-S100-07, P_{n2}, and (b)

strength prediction from the direct strength method in Appendix 1 of AISI-S100-07, P_{n3}. For the direct strength (P_{n3}) method the distortional buckling and corresponding load capacity is ignored, further the critical local buckling load for the section is determined at the actual member length.

For the studied angle member both the effective width (P_{n1}) and direct strength (P_{n3}) are modestly unconservative for stocky angles (Figure 17a); however for intermediate and high local slenderness angles (Figure 17b-d) the direct strength (P_{n3}) predictions follow the nonlinear trends observed in the ABAQUS results, while the effective width method again assumes a linear change in strength as a function of r/t – a trend not observed in the ABAQUS results.
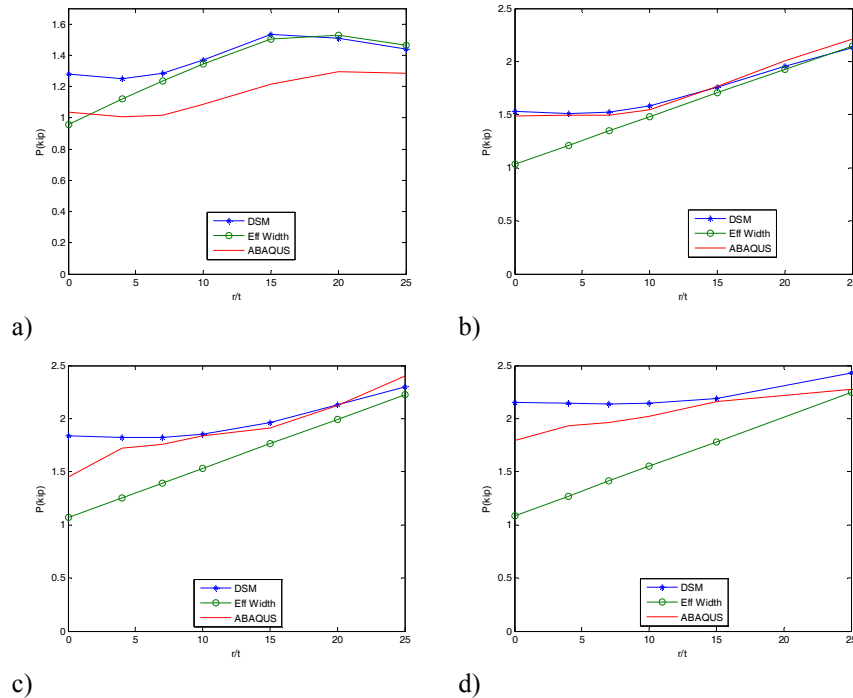
a)

b)

c)   d)

Figure 17: strength of angle members under axial compression.
a) b_o = 0.9 in. wide, b) b_o = 1.6 in. wide, c) b_o = 3.6 in. wide, d) b_o = 7.5 in. wide

5   Preliminary Recommendations for design

Further study and comparison with testing is warranted, nonetheless the lack of any restriction on corner radius in the effective width method of AISI-S100-07

merits at least preliminary recommendations. It is recognized in the studies herein that the normalized corner radius r/t and the ratio of the area in the corners to the area in the flats, which is proportional to r/b, are both influential in determining when existing methods become systematically unconservative. However, r/t has greater influence (and simplicity) and is thus the focus of the simple recommendations provided herein.

It is recommended that the AISI-S100-07 main specification B1 limits be expanded to include a limit of $r/t < 10$. For $r/t > 10$ this would force the engineer to use rational analysis. If effective width method's are still desired for high r/t, then use of the reduced k method would be appropriate at least up to $r/t = 20$. Thus, it is recommended that $k_{reduced}$ be explicitly added to the AISI-S100 commentary discussion of the new $r/t < 10$ limit.

Based on the results presented here it is recommended that for the AISI-S100-07 Appendix 1 direct strength method that the current pre-qualified limit of $r/t < 10$ be liberalized to $r/t < 20$. At the same time, the commentary should be revised to include commentary consistent with Section 2, discussing why upper limits on r/t must still exist, even in the direct strength method.

6   Conclusions

The formation of cold-formed steel cross-sections requires round corners at the locations of plate bends. The effective width method of member strength determination, as implemented in AISI-S100-07, assumes all corners remain fully effective regardless of their size or slenderness. This approach is demonstrated to be unconservative by comparison to ABAQUS collapse analysis conducted for stiffened elements, unstiffened elements, and members comprised of stiffened elements (tubes) and unstiffened elements (angles); particularly for r/t in excess of approximately 10. A "reduced k method" which provides a simple correction to the plate buckling coefficient employed in the effective width method is demonstrated to improve the accuracy even for r/t as high as ~ 20; however, since it also applies no reduction on the corners it eventually becomes unconservative as well. The direct strength method of member strength determination as implemented in AISI-S100-07 Appendix 1 is also compared to the ABAQUS collapse analysis. The method generally provides good predictions for the corner radius studied. In particular, nonlinear trends in capacity as a function of r/t are replicated in the direct strength method approach. It is recommended that the existing effective width method approach in AISI-S100-07 be limited to $r/t < 10$ and that the pre-qualified limits in the direct strength method (AISI-S100-07 Appendix 1) be liberalized to $r/t < 20$.

References

ABAQUS. ABAQUS/Standard Version 6.7-3. Providence, RI: Dassault Systèmes, http://www.simulia.com/, 2007.

AISI-S100-07. North American Specification for the Design of Cold-Formed Steel Structures. American Iron and Steel Institute, Washington, D.C., AISI-S100. 2007.

EN-1993-1-3. Eurocode 3: Design of Steel Structures, Part 1-3: Supplementary rules for cold formed thin gauge members and sheeting. European Committee for Standardization, CEN, Brussels.

Gao, T., Moen, C. D., *The cold work of forming effect in structural steel members.* International Collquium, Stability and Ductility of Steel Structures, Rio de Janeiro, Brazil, 2010.

Marsh, C., *Influence of bend radii on local buckling in cold formed shapes.* ASCE, Journal of Structural Engineering, 1997, 123(12): p. 1686-1689

Moen, C.D., Igusa, T., Schafer, B.W., *Prediction of residual stresses and strains in cold-formed steel members*, Journal of Thin-Walled Structures, 2008

Schafer, B.W. and T. Peköz, *Computational modeling of cold-formed steel: Characterizing geometric imperfections and residual stresses.* Journal of Constructional Steel Research, 1998. 4**7**(3): p. 193-210.